Title: Systematic studies on the dynamics, intermolecular interactions and local structure in the alkyl and phenyl substituted butanol isomers

Author: Barbara Hachuła, Joanna Grelska, Natalia Soszka, Karolina Jurkiewicz, Andrzej Nowok, Anna Z. Szeremeta, Sebastian Pawlus, Marian Paluch, Kamil Kamiński

Citation style: Hachuła Barbara, Grelska Joanna, Soszka Natalia, Jurkiewicz Karolina, Nowok Andrzej, Szeremeta Anna Z., Pawlus Sebastian, Paluch Marian, Kamiński Kamil. (2021). Systematic studies on the dynamics, intermolecular interactions and local structure in the alkyl and phenyl substituted butanol isomers. "Journal of Molecular Liquids" ((2021), art. no. 117098), doi 10.1016/j.molliq.2021.117098

Journal of Molecular Liquids xxx (xxxx) xxx

Contents lists available at ScienceDirect

Journal of Molecular Liquids

journal homepage: www.elsevier.com/locate/molliq

Systematic studies on the dynamics, intermolecular interactions and local structure in the alkyl and phenyl substituted butanol isomers

B. Hachuła [a,b,*], J. Grelska [b,c], N. Soszka [a,c], K. Jurkiewicz [b,c,*], A. Nowok [b,c], A.Z. Szeremeta [b,c], S. Pawlus [b,c], M. Paluch [b,c], K. Kaminski [b,c]

[a] Institute of Chemistry, University of Silesia in Katowice, Szkolna 9, 40-006 Katowice, Poland
[b] Silesian Center for Education and Interdisciplinary Research, 75 Pulku Piechoty 1a, 41-500 Chorzow, Poland
[c] August Chelkowski Institute of Physics, University of Silesia in Katowice, 75 Pulku Piechoty 1, 41-500 Chorzow, Poland

ARTICLE INFO

Article history:
Received 31 March 2021
Revised 20 July 2021
Accepted 24 July 2021
Available online xxxx

ABSTRACT

In this paper, we have studied local structure, interactions scheme and molecular dynamics of series of aliphatic butanol (AB) isomers: n-butanol, *iso*-butanol, *sec*-butanol, and their phenyl counterparts (PhB): 4-phenyl-1-butanol, 2-methyl-3-phenyl-1-propanol, and 4-phenyl-2-butanol by means of X-ray diffraction (XRD), Fourier transform infrared (FTIR), and broadband dielectric spectroscopy (BDS) methods. XRD demonstrated that aside from the main peak related to the nearest-neighbour intermolecular correlations, there is a strong pre-peak at low scattering vector range for ABs, while for PhBs, this diffraction feature was weakly visible or not detected at all. At first sight, it suggests that molecules in aliphatic alcohols tend to associate and form medium-range order, while PhBs can be considered as disordered, simple liquids. However, further thorough FTIR and BDS spectroscopy investigations have shown that the phenyl moiety affects only slightly the degree of association and does not influence the strength of H-bonds in aromatic alcohols. What is more, PhBs are characterized by a similar Kirkwood factor ($g_k \gg 1$) to the ABs. 4-phenyl-2-butanol is characterized by the greatest $g_k \sim 3.7$ among all studied herein alcohols, indicating a strong correlation between dipole moments and the formation of nanoassociates of chain-like topology in its structure. Combining results obtained from different experimental techniques, we pointed out that there are clear differences in dynamic and static properties between primary and secondary alcohols, including medium- and short-range order, variation in the strength of H-bonds and distribution of these types of interactions, the enthalpy of dissociation process, the glass transition temperature, and Kirkwood factor, irrespective of the presence of steric hindrance posed by the phenyl moiety. Results discussed in this paper clearly demonstrated that a superficial analysis of standard diffraction patterns, which are often the first step to probe the structure of materials, may lead to wrong conclusions. That is why complementary techniques must be applied together to understand the structure and behavior of assembling liquids.

1. Introduction

Supramolecular self-assembly is a phenomenon underlying the structure, thermodynamics, and physicochemical properties of various systems, and above all, the fundamental processes occurring in living organisms [1]. The driving forces responsible for the association of molecules are weak interactions, i.e., electrostatic and van der Waals forces, π-π stacking, or hydrogen bonding, which entail the formation of supramolecular aggregates with high stability. The molecular aggregation has been intensively explored in aqueous, and more generally, liquid binary mixtures due to their importance in various biological, chemical, and engineering processes, such as protein folding, membrane assembling, electrochemical charging, and heterogeneous catalysis [2–8]. By manipulating the composition of a binary mixture (e.g., protic versus aprotic or polar versus non-polar solvent), one may induce strong variation in the tendency to associate or enforce molecules to form self-assembles of different architecture. In fact, prediction and characterization of the static and dynamic properties of nanoassociates in solutions are possible because there are many experimental methods dedicated especially to study such systems. A very useful technique is the solution-state infrared spectroscopy, which supplies structural information on the supramolecular association upon dilution of the studied system (e.g., how the system

* Corresponding authors at: Silesian Center for Education and Interdisciplinary Research, 75 Pulku Piechoty 1a, 41-500 Chorzow, Poland.
E-mail addresses: barbara.hachula@us.edu.pl (B. Hachuła), karolina.jurkiewicz@us.edu.pl (K. Jurkiewicz).

https://doi.org/10.1016/j.molliq.2021.117098
0167-7322/

changes with the solvent concentration and how the molecules interact with each other in different kinds of solutions) [9–14]. This method also enables researchers to determine the degree of association, the solvent character, the solute concentration, and the steric hindrance effects. On the other hand, the dynamic and static light scattering (DLS, SLS) measurements may provide the distribution and the mean size of the mesoscale aggregates as well as their molecular weight in solutions [15,16,17]. However, it must be stressed that the studies in solutions do not provide the information on the 'true' self-assembly of a neat compound since the molecular clustering in such a case is affected, or sometimes even triggered, by the presence of a solvent.

In the case of highly viscous neat compounds, the investigation of the supramolecular self-assembly is more difficult since most of the available experimental tools lose power and become insensitive to the molecular association and organization on a scale ranging up to a maximum of a few nanometers. Based on the publication records on this topic, one can state that there are four main pillars of the supramolecular aggregation studies of neat liquids - Fourier transform infrared (FTIR) spectroscopy, X-ray or neutron diffraction (XRD or ND, respectively), broadband dielectric spectroscopy (BDS), and molecular dynamics simulations. XRD/ND allows revealing many features of the intermolecular structure of liquids. In many systems forming the medium-range order and mesophases, except for the main diffraction peak, related to the short-range correlations between the nearest-neighbor molecules, an additional feature, so-called pre-peak, may be observed. The pre-peak's parameters (i.e., intensity, width, and position) are sensitive to various physical conditions (e.g., temperature and pressure) and provide important information about the concentration, geometry, size and degree of order of the supramolecular structures in the liquid/glass phases, especially when supported by the pair distribution function analysis and molecular modelling [18,19,20]. In turn, the BDS method delivers details on the long-distance correlation between the dipole moments in associating liquids, reflected in the value of the static permittivity or Kirkwood correlation factor, g_k. The value of g_k is a fingerprint of the molecular organization in liquids. According to the Dannhauser model applied for monohydroxy alcohols, the value of g_k allows to distinguish between chain- and ring-like organization of H-bonds in supramolecular clusters [21]. A piece of valuable knowledge about the static and dynamic properties of the supramolecular structures may also be provided by the analysis of the position and the amplitude of the anomalous Debye relaxation process, observed in self-assembling liquids, especially in alcohols [1]. Interestingly, for this group of compounds with highly polar units, IR spectroscopy also delivers extremely valuable data about the character and the nature of directional H-bonds implying the molecular clustering. Nevertheless, despite multilateral and complex approaches to understanding the supramolecular self-assembly and nanostructuring in neat viscous alcohols, many issues, including the influence of a steric hindrance on the affinity to form H-bonded clusters and their architecture, as well as on the dielectric properties, remains unsolved.

In this paper, we systematically study a series of structural alkyl butanol isomers: n-butanol (nBOH), *iso*-butanol (iBOH), *sec*-butanol (sBOH), and their phenyl counterparts: 4-phenyl-1-butanol (4Ph1BOH), 2-methyl-3-phenyl-1-propanol (2M3Ph1POH), and 4-phenyl-2-butanol (4Ph2BOH), in neat forms, to recognize the influence of steric hindrance in the form of the phenyl ring as well as the location of the hydroxyl unit in the alkyl chain with respect to the phenyl ring on the self-assembly phenomena. We used three main experimental methods, XRD, FTIR, and BDS, providing complementary data on the self-organization of molecules, to create a clearer picture of their behavior in the context of the self-assembly. Especially, the degree of association via H-bonds, their strength and distribution, the degree of the intermolecular order on the short- and medium-range scale, the size of the supramolecular clusters and the dielectric relaxation processes were studied.

2. Materials and methods

Aliphatic series of isomers of butanols: n-butanol, *iso*-butanol, *sec*-butanol, as well as their phenyl counterparts: 4-phenyl-1-butanol, 2-methyl-3-phenyl-1-propanol, and 4-phenyl-2-butanol, of the purity higher than 98% were supplied from Sigma Aldrich. The chemical structure of the studied alcohols is shown in Scheme 1.

2.1. Broadband dielectric spectroscopy (BDS)

The dielectric properties of the studied butanols were investigated at ambient pressure using BDS in a temperature range extending 100 K. The dielectric measurements were performed within the frequency range from 10^{-2} to 10^{6} Hz with a Novocontrol spectrometer, equipped with Alpha Impedance Analyzer with an active sample cell and Quatro Cryosystem for temperature stabilization better than ± 0.2 K. The capacitor was built from two stainless steel electrodes, 15 mm in diameter, distanced with two 100 μm thick glass fibers and sealed within a Teflon ring.

2.2. X-ray diffraction (XRD)

X-ray diffraction measurements for the studied alcohols were performed on a Rigaku-Denki D/MAX RAPID II-R diffractometer equipped with a rotating Ag anode, an incident beam (002) graphite monochromator, and an image plate in the Debye–Scherrer geometry. The samples were measured at room temperature (*RT* = 293 K) and around the glass transition temperature (T_g ± 5 K). The temperature was controlled using an Oxford Cryostream Plus and Compact Cooler. Samples were measured in glass capillaries with a diameter of 1.5 mm. The collected two-dimensional diffraction patterns were converted into one-dimensional intensity data versus the scattering vector, $Q = 4\pi(sin\theta)/\lambda$, where 2θ is the scattering angle and the wavelength of the incident beam, λ, is equal to 0.56 Å. The low-*Q* XRD data up to ~1.7 $Å^{-1}$ were fitted with pseudo-Voigt functions using the Fityk software to determine the diffraction peak's position and full width at half maximum, *FWHM*.

2.3. Fourier transform infrared (FTIR) spectroscopy

FTIR spectroscopy measurements of the studied alcohols were carried out on a Thermo Scientific Nicolet iS50 spectrometer. High-temperature (*HT*; from *RT* to 368–388 K) FTIR spectra were measured using GladiATR accessory (Pike Technologies) coupled with a FTIR spectrometer in the range 400–4000 cm^{-1} (16 scans; spectral resolution 2 cm^{-1}). The absorption signals were recorded every 2 K (nBOH) or 5 K (iBOH and sBOH) from *RT* to 388 K (nBOH), 378 K (iBOH), and 368 K (sBOH). Low-temperature (*LT*; from *RT* to the glass transition temperature, T_g) spectra were obtained applying a Linkam THMS 600 temperature controller (Linkam Scientific Instruments Ltd, Surrey, UK) over a wavenumber range 800–4000 cm^{-1} (16 scans; spectral resolution 4 cm^{-1}). The cooling rate was 10 K/min, and the temperature stabilization accuracy was 0.1 K. The preparation of liquid samples for the *LT*-FTIR measurements was presented in our previous work [22]. A solution-state FTIR spectroscopy experiment was performed to estimate the dimension of H-bonded aggregates in the alcohols. A wide range of concentrations of alcohol solutions in carbon tetrachloride

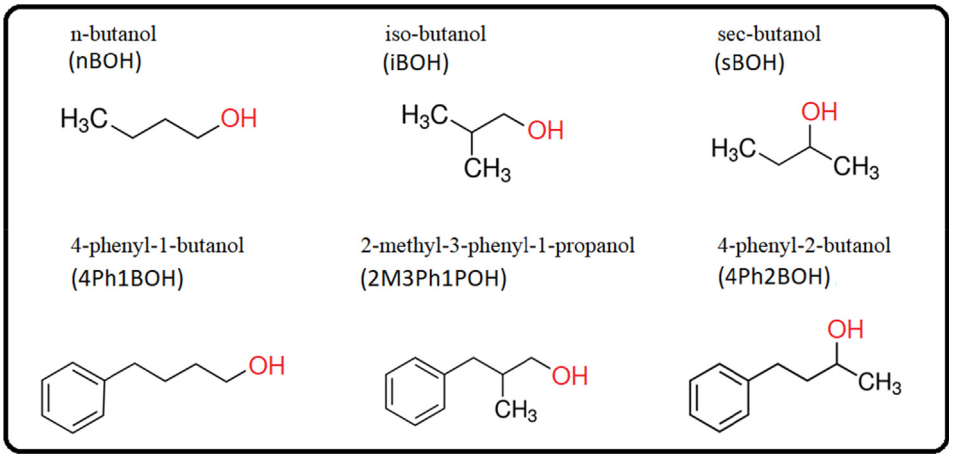

Scheme 1. The chemical structure of the alkyl and phenyl substituted butanol isomers.

(CCl_4), i.e., 0.0005–0.1 M, was prepared using a serial dilution method. FTIR spectra of pure solvent and alcohol solutions were measured in the frequency range 400–4000 cm^{-1} using a transmission solution cell with KBr windows and a path length of 1.03 mm. 16 scans with a spectral resolution of 4 cm^{-1} were averaged for each sample. The final FTIR spectra of alcohol solutions were obtained by subtracting the spectrum of the pure solvent from the measured absorption spectrum and applying baseline correction. The OH stretching band deconvolution was performed using the MagicPlot software (version 2.9.3, MagicPlot Systems LLC, Saint Petersburg, Russia). Firstly, the decomposition of the ν_{OH} band occurring between 3700 and 3050 cm^{-1} involved the curve fitting of the ν_{OH} band with the use of several Gaussian functions, adjusting their intensity, position, and width. Secondly, the free OH band, appearing between 3650 and 3550 cm^{-1}, was obtained by subtracting the deconvoluted H-bonded OH band from the original ν_{OH} band. Then, the peak fitting of the free OH band was performed. All spectral parameters were left 'free' during the fitting procedure.

3. Results and discussion

1 The static structural features of alkyl butanols and their phenyl counterparts

It is known for a half-century that diffraction data are sensitive to the local structure and the medium-range order in alcohols. The static scattering pattern reveals a pre-peak (*PP*) at $Q \approx 0.5$ $Å^{-1}$ for various alcohols, which has recently been clearly confirmed as arising due to the assembly of molecules in aggregates via H-bonds [18]. The pre-peak in the total structure factor becomes the main peak in the partial structure factor for hydroxyl groups. It simply means that there are structural correlations between the neighbouring skeletons of OH groups entailing the formation of the medium-range order. The pre-peak feature has been experimentally observed in XRD and ND data [22,23,24] as well as predicted by computer simulations [19,25,26,27,28] for many alcohols, including butanols. The modeling of the structure of fluid nBOH, iBOH and sBOH revealed that they are characterized by associates with the mainly chain-like architecture of H-bonds [29,30].

Our XRD data for all studied ABs, nBOH, iBOH, and sBOH, exhibit the characteristic pre-peak feature at $Q \approx 0.56$, 0.64, and 0.7 $Å^{-1}$ at *RT*, respectively (see Fig. 1), being the evidence of the supramolecular association and structuring of the molecules on the medium-range scale. The main diffraction peak (*MP*), reflecting the nearest-neighbour, short-range intermolecular correlations, appears at $Q \approx$ 1.44, 1.37, and 1.3 $Å^{-1}$ at *RT* for nBOH, sBOH, and iBOH, respectively. According to previous XRD and modeling studies, the first

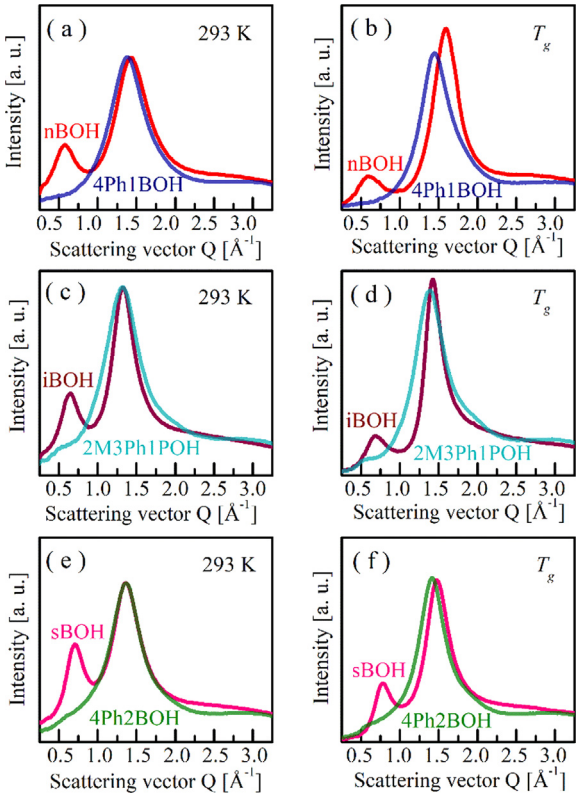

Fig. 1. XRD patterns of the studied alcohols in the low scattering vector range, measured at *RT* and around T_g. Data of alkyl butanols were normalized to the intensity at the high scattering vector range (> 6 Å). Their phenyl counterparts were normalized to the main-peak intensity of the corresponding alkyl butanol pattern at *RT*.

coordination shell for O-O distance of nBOH has the coordination number around 2 [31]. That means the supramolecular clusters in nBOH are rather small, composed of a few molecules at *RT*. Since up to now there is no consensus regarding the detailed size and number of assembled molecules in the clusters from the diffraction data for these alcohols, here we decided to determine only their basic structural parameters assuming the quasi-crystalline model of the structure. Namely, these are: the average nearest-neighbour intermolecular distance, d_{MP}, calculated from the position of the *MP* using the Bragg equation $d = 2\pi/Q$; the average

separation distance between neighbouring associates (OH-skeletons), d_{PP}, calculated from the position of the pre-peak; the coherence lengths related with the short-range and medium-range order, L_{MP}, and L_{PP}, respectively, calculated from the peak *FWHMs* using the formula $L = 2\pi/FWHM$. From the comparison of the static structural parameters set together in Fig. 2, one can see the following differences between the studied ABs at *RT*: (*i*) the d_{MP} distance increases in the following order: nBOH, then sBOH, and the most branched iBOH; (*ii*) in turn, the d_{PP} is the greatest for nBOH, and the shortest for sBOH. It is worth mentioning that the determined distances are related to the geometry of the molecules, their packing abilities, and the location of the OH group, e.g., molecules of nBOH are longitudinal, unbranched, with terminal OH group, which directly implies small distances between them in the direction of the short molecular axis and large distances between neighbouring OH skeletons assuming the chain-like model.

Considering the characteristic lengths of the short and medium-range order, one can notice that: (*i*) nBOH is the least ordered, sBOH is more ordered, and iBOH is the most ordered on the short-range scale based on the L_{MP} value (~17 ± 0.5 Å); (*ii*) the range of the medium-range correlations L_{PP} changes inversely proportional to d_{PP}, which means the greatest intermolecular correlations arise in secondary alcohol sBOH (~21 ± 0.5 Å), shorter in iBOH, and the shortest (~17 ± 0.5 Å) in nBOH (see the panel d of Fig. 2). The last dependency also correlates with the pre-peak intensity – it has the higher amplitude for sBOH and the lowest for nBOH.

Interestingly, the XRD data for 4PH1BOH, 2M3P1POH, and 4PH2BOH, containing phenyl group, do not display the clear presence of the specific pre-peak (see Fig. 1). They look typical for 'ordinary', non-associating liquids with only one pronounced peak at $Q \approx 1.35$ Å^{-1}. However, after a closer look at the XRD patterns for 2M3P1POH and 4PH2BOH a residual bump may be identified at the pre-peak position for their alkyl counterparts, which may be the fingerprint of a weak self-organization of molecules. Despite the fact that the pre-peak is a highly complex feature appearing due to different partial atom-atom contributions to the total diffraction intensity [29], the absence of the pre-peak usually means that there is no structural order between the supramolecular clusters. Thus, the attaching the phenyl ring to the molecules of the studied alcohols suppresses the longer intermolecular correlations and disturbs the medium-range structuring. Moreover, the short-range order seems to be also affected by the presence of steric hindrance in the form of the phenyl group. The determined L_{MP} values are smaller for aromatic alcohols than for their alkyl counterparts, especially at temperatures around T_g (e.g., L_{MP} = 12 ± 0.5 Å for 2M3Ph1POH versus ~23 ± 0.5 Å for iBOH, see the comparison in panel c of Fig. 2). These results fully agree with previous conclusions for phenyl alcohols showing that attaching the phenyl ring to a molecule disturbs the nanoscale organization through H-bonding and hinders the formation of the supramolecular associates [32].

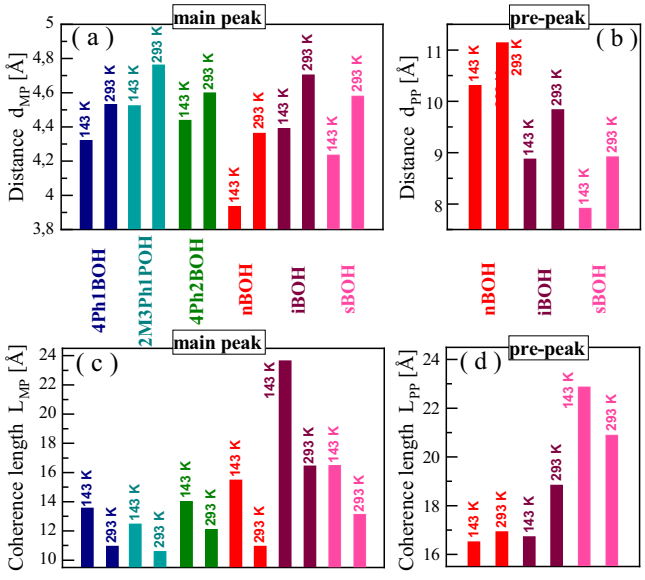

Fig. 2. The average intermolecular distances determined from the positions of the main diffraction peak, d_{MP}, and the pre-peak, d_{PP}, as well as the coherence lengths L_{MP}, and L_{PP}, calculated from the *FWHMs* of these peaks, respectively.

The highest value of L_{MP} (~14 ± 0.5 Å) among PhBs around T_g was obtained for secondary 4Ph2BOH. It is worth stressing that the static structural features estimated for 4Ph1BOH and 4Ph2BOH based on the analysis of the standard diffraction patterns are consistent with the results of the analysis of the structure factors and the pair distribution functions performed in our previous paper [33]. It was concluded that 4Ph1BOH displays a more disordered 'liquid-like' structure compared to 4Ph2BOH, and suggested a more prevalent heterogeneity of H-bonding pattern in the former alcohol. Therefore, further FTIR studies are required to describe in detail the nature of H-bonds in the studied alcohols.

As for the temperature changes, the right panels in Fig. 1 show the diffractograms upon temperature drop to around T_g. The positions of *MP* and *PP* shift towards greater values as the temperature drops. This is related to the decrease of the intermolecular distances in these systems and is the standard temperature effect. The L_{MP} also behaves in a standard manner for each alcohol – it increases with a decrease in temperature. In turn, the L_{PP} decreases with temperature drop for nBOH and iBOH, suggesting a decrease in the degree of the medium-range organization of molecules. What is more, it is clear that the intensity of the pre-peak decreases with decreasing temperature. This observation agrees with previous reports and has been interpreted as a change of the mean number of clusters or/and the nature of the dominant form of clusters [28]. However, this issue is still waiting for a detailed computational explanation.

Summarizing this part, all studied ABs show diffraction patterns with the pre-peak feature, typical for associating liquids where molecules form mesophases and organize on the medium-range scale. The primary butanol – nBOH is characterized by the lower degree of intermolecular order on both the short- and medium-range scale. The branching of molecule in iBOH causes the increase in the range of both short- and medium-range correlations, while the change of the OH group location in secondary sBOH results in the higher degree of the medium-range order. Adding the phenyl group to the molecular structure suppresses both the short- and medium-range order between molecules in PhBs, while secondary 4Ph2BOH is characterized by the greatest coherence length at *LT* and *RT* among the PhBs.

2 The influence of the phenyl ring on the hydrogen-bonding pattern

To probe H-bonds among the studied alcohols, FTIR spectra were firstly measured in the *LT* range. The representative FTIR spectra of alcohols recorded at *RT* and T_g in the region of OH moiety's stretching vibrations (ν_{OH}; 3000–3750 cm^{-1}) are shown in Fig. 3. The temperature evolution of *LT*-FTIR spectra in the ν_{OH} and ν_{CH} frequency ranges is presented in **Figure S1** (see the SI file). At first sight, the OH stretching band of the alcohols consists of two well-separated components, assigned to the stretching vibration of the 'free' (non-H-bonded; ν_{OH}^{free}) and associated (H-bonded; ν_{OH}^{assoc}) hydroxyl groups, respectively. The intensities of these two bands

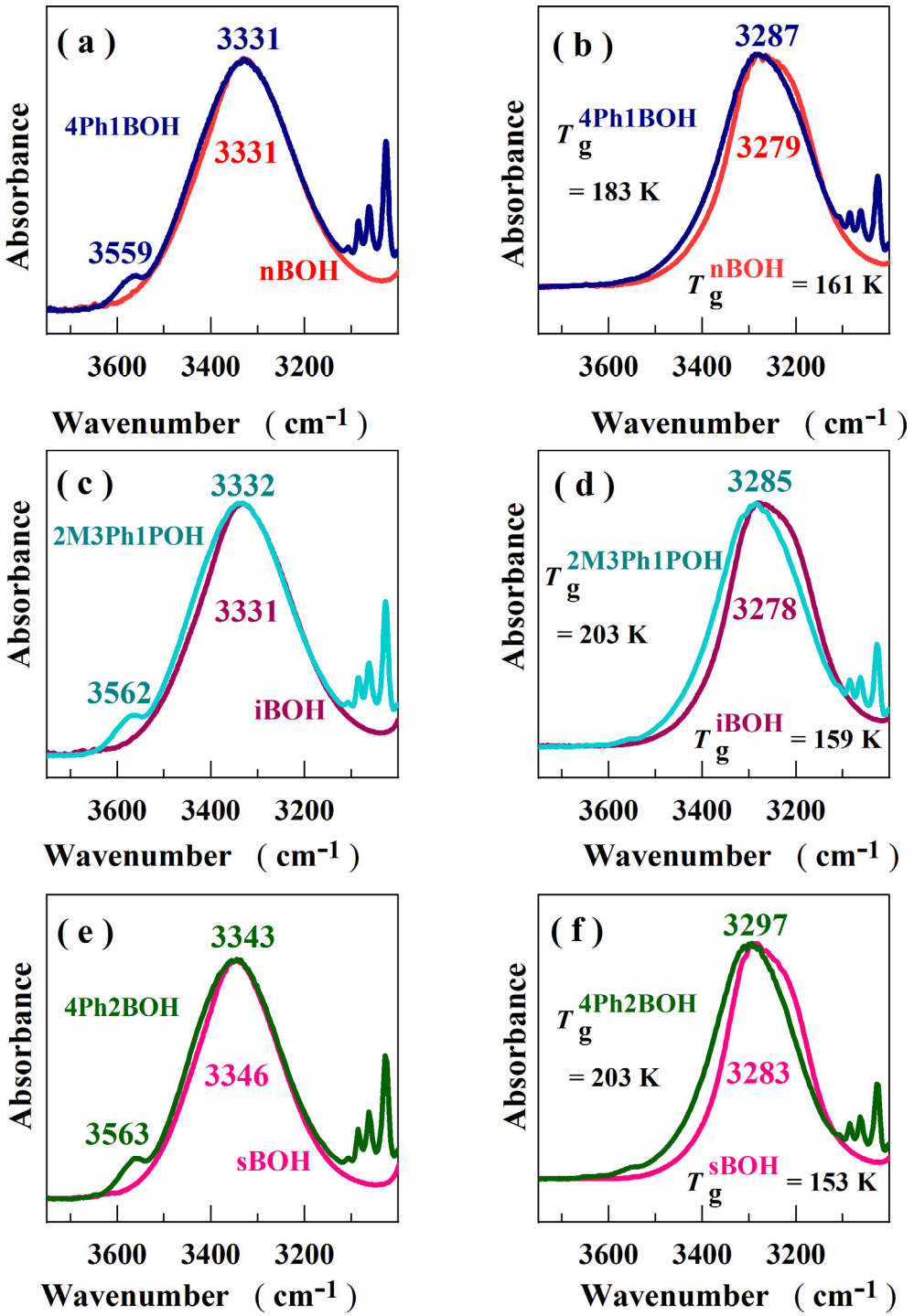

Fig. 3. FTIR spectra of butyl alcohol isomers in the spectral region between 3750 and 3000 cm^{-1} measured at *RT* (panels a), c), e)), and T_g (panels b), d), f)). The spectra were normalized with respect to the absorbance maximum of the OH stretching vibration peak.

vary with temperature. In ABs, only a broad ν_{OH}^{assoc} band appears at *RT*, indicating that nearly all OH groups are H-bonded (Fig. 3). In contrast, aside from the dominant ν_{OH}^{assoc} peak, a weak spectral feature at ~3560 cm^{-1} associated with the free OH vibrations is detected in PhBs. The disappearance of the ν_{OH}^{free} signal with decreasing temperature is due to the undergoing association process of OH groups of aromatic alcohols. As seen from **Table S1** (the SI file), the ν_{OH}^{assoc} band frequency of butanol isomers essentially increases for secondary alcohols (sBOH, 4Ph2BOH) compared to primary ones (nBOH, iBOH, 4Ph1BOH, 2M3Ph1POH) at *RT*. Therefore, the primary butanol derivatives, in which the OH group is attached to a carbon atom with at least two hydrogen atoms, are involved in the stronger H-bond interactions compared to the secondary ones. The presence of phenyl moiety in butyl alcohols has no impact on the strength of the H-bonds at *RT* since the position of the ν_{OH}^{assoc} differs only by 1–3 cm^{-1} (within the resolution of spectrometer) with respect to their aliphatic counterparts. As temperature decreases, the ν_{OH}^{assoc} peak position shifts to lower wavenumbers in each studied system. This well-known effect is an indicator of the OH-bond strength weakening due to the forma-

tion of stronger H-bond interactions. At T_g the similar correlations regarding the ν_{OH}^{assoc} peak position and the OH group's location in the butanol molecules are observed, i.e., the H-bond strength in butanol isomers is the lowest for secondary alcohols. Comparing the ν_{OH}^{assoc} peak positions for aliphatic and aromatic compounds, again the relatively weak influence of the steric hindrance (the benzene ring) on the H-bond strength is noticed for primary butanols. The more considerable steric effect is observed for secondary alcohols, i.e., the difference of the ν_{OH}^{assoc} band frequency reaching 14 cm^{-1} is detected for sBOH versus 4Ph2BOH at T_g. That simply means that from the macroscopic point of view, the association process in butanol alcohols depends mainly on the location of the OH functional group in relation to the carbon skeleton and less on the steric effect introduced by the phenyl moiety.

To gain more information about the H-bonding pattern in the studied alcohols, further analysis of the OH stretching vibration bandwidth (the full-width at half-maximum, *FWHM*) was performed. It turned out that the change of the position of the OH group in butanol skeletons (primary versus secondary ones) influences the OH bandwidth, i.e., the *FWHM* value decreases in the following manner: nBOH > iBOH > sBOH and 4Ph1BOH > 2M3Ph1POH > 4Ph2BOH, at *RT* and T_g (see **Table S1**). This means that the *FWHM* of the ν_{OH}^{assoc} band for primary butanols is larger than for their secondary isomers. The results shown in **Table S1** also indicate that in each pair of alkyl - aromatic butanol isomers, the phenyl derivative exhibits a higher *FWHM* (4Ph1BOH > nBOH, 2M3Ph1POH > iBOH, 4Ph2BOH > sBOH), which means a more inhomogeneous distribution of its H-bonding network. When the temperature drops, the *FWHM* is steadily reduced for all alcohols. This is due to the growth in the homogeneity of H-bonding interactions because of the decreasing mobility of alcohol molecules and the possible extension of the aggregates. This effect is accompanied by the increase of the integral intensity of the ν_{OH}^{assoc} bands on cooling due to the increasing population of H-bonded molecules. In contrast to PhBs, the OH stretching lines of ABs have a slightly antisymmetric contour, suggesting that at least two distinguishable components in the energy distribution of H-bonded molecules occur. Further *HT*-FTIR measurements for butyl alcohols were performed to quantify the activation barrier for dissociation using van't Hoff equation:

$$lnK = \frac{-\Delta H_D}{RT} + \frac{\Delta S}{R} \qquad (1)$$

where ΔH_D and ΔS are activation enthalpy and entropy of dissociation process, respectively.

Figure S2 shows the representative *HT*-FTIR spectra of butyl alcohols in the region of the ν_{OH} and ν_{CH} bands. As can be seen, heating of the alcohol samples causes the growth of intensity of the ν_{OH}^{free} signal due to breaking of the O-H···O bonds (the dissociation process) and the blue-shift (shift to higher wavenumbers) of the ν_{OH}^{assoc} band (~3600–3050 cm^{-1}), which indicates the weakening of H-bonding interactions (**Figure S2**). This effect is accompanied by a decrease in intensity and a broadening of the ν_{OH}^{assoc} band. To calculate the population of non-associated and associated molecules, the integrated intensities of free (A_{free}) and H-bonded (A_{assoc}) OH bands were estimated. Based on the A_{free} /A_{assoc} ratio, the equilibrium dissociation constant, K_D, was evaluated. Further, the K_D values were plotted versus reciprocal temperature and fitted to the van't Hoff equation to calculate ΔH_D of the dissociation process $(O-H)_n \leftrightarrows n(O-H)$. From Fig. 4 it follows that ΔH_D varies from 9.50 kJ mol^{-1} for 4Ph1BOH to 23.21 kJ mol^{-1} for sBOH. Surprisingly, the highest ΔH_D values were obtained for secondary alcohols in both series ABs and PhBs. Thus, more energy is needed to break the H-bonds in these alcohols compared to their primary isomers, probably due to the larger homogeneity of their H-bonding interactions.

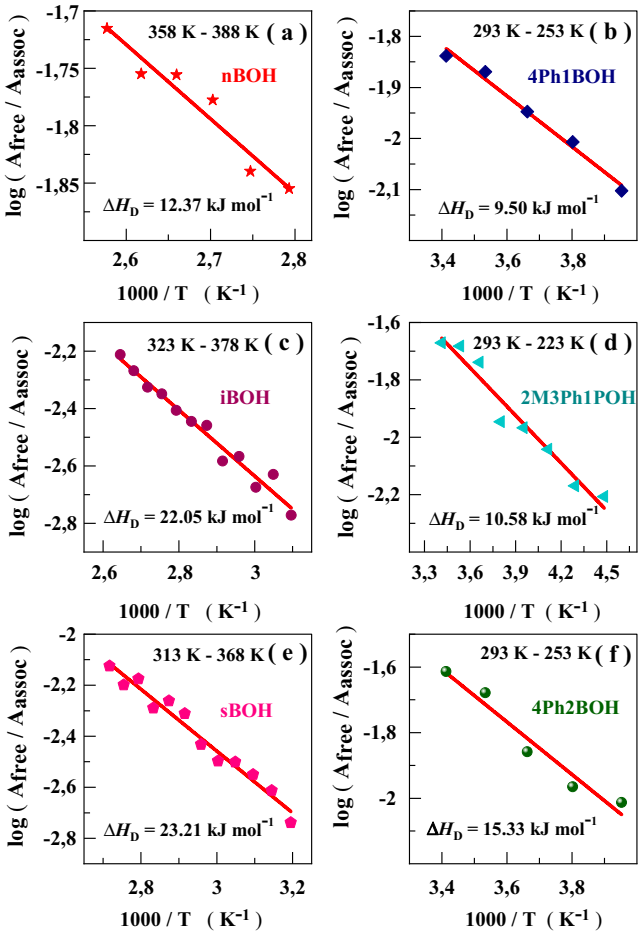

Fig. 4. Van't Hoff plots for the FTIR absorption bands corresponding to the OH bands of ABs and PhBs, used to estimate the dissociation enthalpy between the free and H-bonded OH species.

Finally, FTIR measurements on the solutions of the studied alcohols in CCl_4 were carried out to quantify the average number of H-bonded molecules and the size of the aggregates at *RT* (see the experimental section in the **SI file** for details). According to **Figure S3,** the average number of H-bonded molecules in the supramolecular assemblies, *n*, is between 2 and 3, i.e., $n_{nBOH} = 2.4$, $n_{iBOH,sBOH} = 2.3$ and $n_{2M3Ph1POH} = 3.0$. The *n* value for 4Ph1BOH and 4Ph2BOH, determined in our previous paper [33], was equal to 2.9 and 2.8, respectively. The obtained results suggest that, on average, dimers and trimers are the dominant forms of supramolecular associates in butyl alcohol solutions at *RT*. This rough estimation agrees very well with the data discussed earlier, suggesting that at *RT*, there are mainly small clusters consisted of 2–3 molecules in the studied systems.

In summary, through *LT*- and *HT*-FTIR spectroscopic studies, we found that the spatial arrangement of the OH group in the carbon skeleton of butanol isomers plays an important role in their association process. Analysis of the spectral parameters of the ν_{OH}^{assoc} band reveals that the primary alcohols are characterized by stronger H-bonding interactions and show a larger inhomogeneity of the H-bonding network than their secondary derivatives. On the other hand, the steric effect of a benzene ring on the molecular interactions involving H-bonds in butyl alcohol isomers is rather weak, i.e., alkyl alcohols show a slightly greater strength of H-bond interactions, and their H-bond network is more homoge-

neous (lower *FWHM* values of the ν_{OH}^{assoc} band) compared to the phenyl derivatives. As a result, ABs have higher dissociation constants and form slightly smaller supramolecular clusters in the CCl_4 solution than PhBs. On the other hand, the broadening of the ν_{OH}^{assoc} band of aromatic alcohols may be probably due to the existence of the structural heterogeneities formed by molecules associated additionally via OH···π and/or CH···π interactions [34,35].

3 The dielectric response of the self-assembled butanols and their phenyl derivatives

As a final point of our investigations, dielectric measurements were carried out on the studied alcohols. In the loss spectra of each AB, one can easily identify a dominating process, called 'Debye relaxation', which is characterized by a unique characteristic exponential shape (see Fig. 5). In literature, the Debye mode is considered as originating from the mobility of/within the H-bonded supramolecular structures. Interestingly, the intensity of this mode is very similar for all three aliphatic alcohols. It is worth mentioning that in these compounds also the structural 'α' process can be detected. It is reflected as a change of the slope of the high-frequency side of the dominant Debye peak - so-called 'excess wing'. In addition, the secondary relaxation processes become detectable in the close vicinity and below the T_g for ABs. Interestingly, for PhBs the picture is markedly different. As can be seen from the loss spectra in Fig. 5**,** for 4Ph1BOH, 2M3Ph1POH, and 4Ph2BOH, only a single, slightly stretched relaxation mode is observed together with a poorly visible secondary process at higher frequencies. Taking into account the results presented in references [32 and 33], one can assume that, in fact, the Debye process gives the main contribution to the dominant relaxation mode observed in the loss spectra of these alcohols. The structural relaxation mode in these alcohols is too close to the Debye process to be experimentally detected in the loss spectra. Therefore, for the purpose of this paper, we will label the observed main relaxation peak as the 'Debye-like' process.

To get an insight into dynamics of the studied alcohols and determine the temperature evolution of the structural, Debye and Debye-like relaxation times above the T_g, the collected loss spectra were fitted to a combination of either one (for PhBs) or two Havriliak-Negami (HN) functions (for ABs) with an additional conductivity term [37]:

$$\varepsilon^*\left(\bar{\omega}\right) = \frac{\sigma_{dc}}{\varepsilon_0\,\bar{\omega}} + \varepsilon_\infty + \frac{\Delta\varepsilon}{\left[1+\left(i\,\bar{\omega}\,\tau_{HN}\right)^{\alpha_{HN}}\right]^{\gamma_{HN}}} \tag{2}$$

where: ε_0 is the vacuum permittivity, σ_{dc} is the direct current conductivity, ε_∞ is the permittivity at high frequency, $\Delta\varepsilon$ is the dielectric relaxation strength, τ_{HN} is the HN relaxation time, which can be used to determine the relaxation time of the main process, τ_{max}, α_{HN} and γ_{HN} are the shape parameters representing symmetric and asymmetric broadening of the loss spectrum ($0 < \alpha_{HN}, \gamma_{HN} < 1$), and $\bar{\omega}$ is the angular frequency.

Inverse temperature dependence of τ_{max} for each relaxation process in studied herein compound is presented in Fig. 6. At first sight, it can be noted that $\tau(T)$ of the Debye-like process in PhBs is much steeper with respect to the temperature evolution of the relaxation times of the Debye mode in ABs. Moreover $\tau_\alpha(T)$ dependences also differ from each other indicating variation in the T_g along with the chemical structure of the butanol isomers. To quantify this effect, we calculated the glass transition temperatures from the presented data. Note that T_g was defined as a temperature at which the relaxation time determined for the α process, τ_α, (for ABs) and the main Debye-like process, τ_{main}, (for PhBs) is equal to 100 s. The values of T_g are presented in Table 1. It should also be stressed that since the determination of the T_g from dielectric data is prone to over or underestimation due to large uncertainty in the determination of the structural relaxation times, further differential scanning calorimetry (DSC) measurements were carried out to verify the accuracy of our analysis. The representative thermograms are presented in **Figure S4** in the **SI file**. We compared also DSC results taken from the literature [36] (see Table 1). It was found that there is quite a good agreement (within a few K) between the T_gs estimated from both experimental techniques. Finally, one can state that that calorimetric T_gs of aromatic alcohols are much higher (T_g = 179, 198 and 203 K for 4Ph1BOH, 2M3Ph1POH and 4Ph2BOH, respectively) with respect to the aliphatic compounds (T_g = 111.6, 113 and 120 K for nBOH, iBOH and sBOH, respectively). What is more, it becomes clear that T_g of secondary alcohols is slightly higher than that of their primary counterparts. The variation in the vitrification temperatures for phenyl derivatives of butanols must be related to the higher molecular weight of these compounds and the presence of aromatic moiety allowing the formation of additional, weak H bonds.

In the next step of analysis of dielectric data, we applied a model developed by Fröhlich [38] to evaluate the change in the molar entropy, ΔS, induced by an external electric field, E, in the studied systems. According to this approach, this parameter can be determined following the temperature evolution of the static permittivity using the equation given below:

$$\frac{\Delta S(T)}{E^2} = \frac{S(T,E) - S_0(T)}{E^2} = \frac{\varepsilon_0}{2}\frac{d\varepsilon_s}{dT}(T) \tag{3}$$

It was already shown by Jadżyn and Świergiel [39] that in the case of butanols, the ordering of polar molecules by an electric field leads to the decrease in the entropy of liquid ($\Delta S < 0$), being a consequence of negative slope of $d\varepsilon'/dT$ function. This kind of analysis revealed that nBOH and sBOH form chain-like structures [39]. The results presented in **Figure S5** indicate that a similar conclusion can also be derived for iBOH. Nevertheless, the most interesting

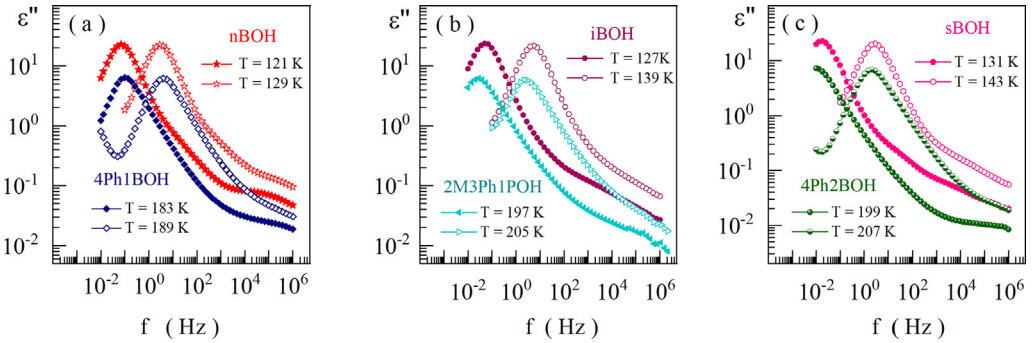

Fig. 5. Comparison of the dielectric loss spectra $\varepsilon''(f)$ measured at similar relaxation times for a) nBOH and 4Ph1BOH, b) iBOH and 2M3Ph1POH, and c) sBOH and 4Ph2BOH.

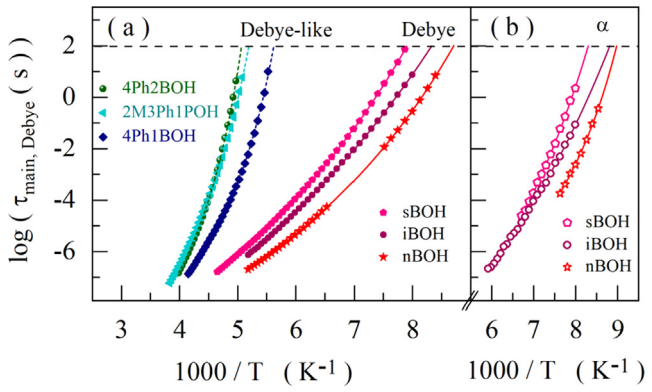

Fig. 6. Relaxation time versus inverse temperature for a) the Debye and Debye-like processes and b) structural process in the aliphatic butanols and their phenyl derivatives.

seems to be a comparison of the outcome of the analysis performed for ABs and their phenyl counterparts. It seems clear from **Figure S5** that the temperature evolution of $d\varepsilon'/dT$ exhibits a negative slope for PhBs, indicating entropy decrease under the influence of electric field in these alcohols. What is more, except for sBOH and 4Ph2BOH, the ΔSV_mE^{-2} versus T dependences obtained for other alcohols collapse on one curve (compare Fig. 7 **a,b,c**). This finding indicates that there are chain-like structures formed in more sterically hindered alcohols as well.

As a final step of our investigations, we evaluated the temperature evolution of the Kirkwood factor, g_k, for alkyl and phenyl butanols (see Fig. 7 **d**). This parameter was calculated from the following equation:

$$g_k = \frac{9k_B\varepsilon_0 MT(\varepsilon_s - \varepsilon_\infty)(2\varepsilon_s + \varepsilon_\infty)}{\rho N_A \mu^2 \varepsilon_s (\varepsilon_\infty + 2)^2} \quad (4)$$

where: k_B is the Boltzmann's constant, ε_0 is the permittivity of vacuum, M is molar mass, ρ is density, N_A is Avogadro's number, μ is molecular dipole moment determined from density functional theory computations. The static permittivity, ε_s, was taken directly from the dielectric data. The methods used to estimate permittivity at infinite frequencies, ε_∞, as well ρ, have been previously described in reference [22]. The data for aliphatic butanols were taken from [40].

As shown in Fig. 7 **d**, all studied alcohols exhibit g_k to be noticeably greater than the unity in the vicinity of *RT*. What is more, g_k systematically grows upon cooling for each alcohol. However, different trends in the changes of g_k with temperature are observed. For ABs, g_k increases sharply at higher temperatures and saturates at around 270 K, much above the T_g, while for aromatic alcohols, except for 4Ph1BOH, it continuously grows in the studied temperature range. The data presented in Fig. 7 **d** also reveal that, beside one unexpected case for 4Ph2BOH, slightly higher or comparable values of g_k were obtained for ABs. This parameter is also larger in secondary alcohols, irrespective of the steric hindrance.

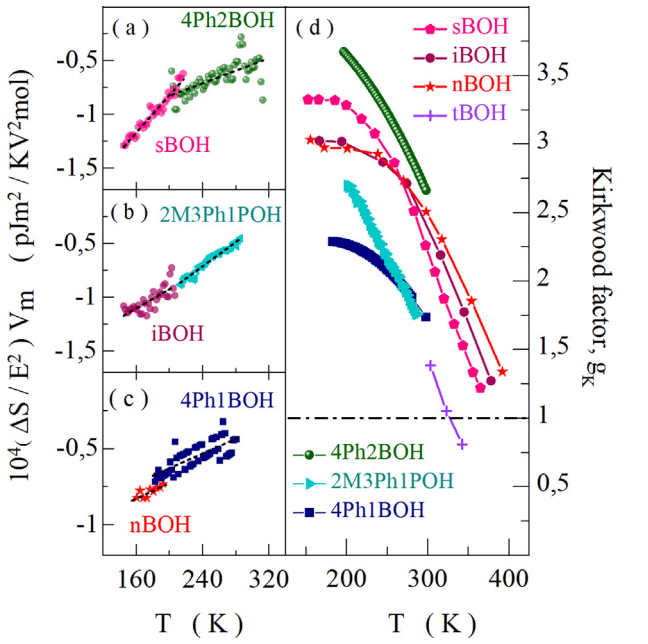

Fig. 7. Temperature dependence of the molar entropy increments induced by the external electric field applied to a) sBOH and 4Ph2BOH, b) iBOH and 2M3Ph1POH, c) nBOH and 4Ph1BOH. d) Comparison of temperature dependences of the Kirkwood factor for the studied butanols.

Both quite unexpected results of the performed analysis of dielectric data demand further thorough discussion. First, it is quite interesting and unexpected that the g_k is much higher in secondary alcohols with respect to the primary ones. As shown in the literature, due to a higher steric hindrance in such systems, generally, chain-ring equilibrium is shifted towards the formation of the cyclic structures that contributes to a significant depression of this parameter. To support this hypothesis, one can recall data reported for 4-methyl-3-heptanol, which revealed a small Debye process in loss spectra and g_k below 1 [41,42]. What is more, one can also refer to a temperature evolution of Kirkwood parameter in tertiary alcohol *tert*-butanol (see Fig. 7 **d**) that was much lower than the unity at high temperature. Nevertheless, as temperature decreased, it became much higher than 1. These two examples suggest that the position of the hydroxyl moiety in the carbon backbone has a strong influence on the architecture of the nanoassociates. It seems that ring-like structures are more preferred in the secondary and tertiary alcohols while chain-like clusters - in the primary ones. However, it is not a rule since in 5-methyl-3-heptanol it was shown that there is a Debye process of slightly lower amplitude with respect to 2-ethyl-1-hexanol. Moreover, this glass former has a rather high g_k. Hence, this system, along with the ones studied herein (sBOH and 4Ph2BOH), clearly indicated that secondary alcohols might predominantly form chain-like associates. To explain the much higher Kirkwood factor for the secondary aliphatic and phenyl derivatives of butanols with respect to the other

Table 1
The values of T_g determined from dielectric data and differential scanning calorimetry (DSC) measurements.

Sample	$T_{g(DSC)}$ (K)	$T_{g(DSC)}$ (K) [36]	$T_{g(Debyelike)}$ (K)	$T_{g(\alpha)}$ (K)
nBOH	111.6	111	–	111.4
iBOH	113	113	–	113.5
sBOH	120	118	–	120.5
4Ph1BOH	179	–	178	178
2M3Ph1POH	198	–	193	193
4Ph2BOH	203	–	197.4	197.5

studied herein samples, one should consider XRD and FTIR data showing the enhanced degree of the intermolecular order and more homogeneous distribution of the H-bonds in these systems. Both factors contribute to better ordering and lower spatial diversity of nanoassociates.

An explanation of the non-intuitive and peculiar variation in g_k in phenyl alcohols with respect to their aliphatic derivatives is a much more difficult issue. Considering structural studies (including ours) and literature reports on the self-assembly processes in similar systems, it is rather expected that due to lower steric hindrance, aliphatic compounds may form larger chain-like associates and thus are characterized by much higher static permittivity and g_k. Interestingly, comparable or larger g_ks have been determined for the phenyl butanols with respect to their aliphatic counterparts, even though in the diffractograms of PhBs there was no pronounced pre-peak being a direct evidence of the formation of the H-bonded assemblies and the nanoscale order. Thus, the diffraction data suggested that the degree of association and ordering is much lower in PhBs. Further FTIR and dielectric studies indicated that this XRD-based picture does not reflect the complex nature of more sterically hindered alcohols. Moreover, the BDS investigations clearly demonstrated that in aliphatic and phenyl derivatives of alcohols, there are self-assemblies of a more probable chain-like architecture. Nevertheless, understanding the extremely high g_k in 4Ph2BOH at the moment is a hard task and has a more speculative character. One can suppose that most likely chain-ring equilibrium of H-bonding clusters is more shifted towards the former architecture in this alcohol. What is more, most probably there are also additional OH$\cdots\pi$ interactions that contribute to larger energy of dissociation in secondary alcohols with respect to the primary ones. These forces may stabilize some specific chain-like molecular architecture that generates high g_k in this alcohol. To verify this hypothesis, one can refer to our previous high-pressure investigations revealing that activation volume for the Debye-like process in secondary alcohols is the highest of all studied alcohols [32]. That may suggest that the size of associates is much larger for 4Ph2BOH with respect to the other phenyl derivatives of butanols. Finally, it should be noted that analysis of the temperature evolution of the Kirkwood factor in the studied system yields explanation of the similar ΔSV_mE^{-2} dependency versus T in nBOH – 4Ph1BOH, iBOH – 2M3Ph1POH, and the deviation reported for sBOH – 4Ph2BOH. It seems that the main source of this experimental finding is related to the variation of the static permittivity during cooling.

The results described above are also quite interesting in view of the recent studies on the self-assembly in ionic liquids (ILs). Briefly, similarly to monohydroxy alcohols (MAs), a spatial organization in ILs is also governed by the amphiphilicity that dominates over Coulombic forces [43]. It was found that with the increasing length of the side alkyl chains attached to the aromatic imidazolium ring, the short-range solvophobic interactions become more important [44,45,46,47]. Interestingly for the aliphatic moiety having more than four carbon atoms, the nanoassocation and nanoordering are triggered. The situation changes as polar H-bonding units such as hydroxyl, thiol, amine, halogen, interfering with amphiphilicity, are introduced to the chemical structure of IL [43]. When the number of polar moieties is low, the competition between both specific interactions induces a disorder in the clustered nanostructure. In the case of a larger number of polar groups, the tricontinuous structure is formed. Hence in some way, these experimental observations are in agreement with the data discussed for MAs. In the studied herein phenyl derivatives of alcohols, the location of both butyl moiety attached to the aromatic unit and OH moiety have a strong influence on the loss of the medium-range order, as evidenced by the collected diffractograms. Simultaneously the clustering process is not affected in a significant way, as it was deduced from the analysis of the Kirkwood factor that reflects the long-distance correlation between dipoles. However, aside from this effect, the location of the OH functional group in the alkyl chain is also an important factor controlling the nanoordering in self-assemblies and eventual loss of the medium-range order, as evidenced by the collected diffractograms. Importantly, simultaneously the clustering process is not affected in a significant way, as it was deduced from the analysis of the Kirkwood factor that reflects the long-distance correlation between dipoles.

4. Conclusions

To summarize, we have investigated the local structure and the molecular network organization in selected aliphatic and aromatic isomers of butanols using XRD, FTIR, and BDS techniques. The main purpose of these studies was to gain a deeper insight into the influence of the steric hindrance introduced by the phenyl moiety and the location of the hydroxyl group on the association process of these alcohols. In the context of the H-bond interaction, the phenyl alcohols received less attention in the literature than aliphatic alcohols, mostly because of the common belief that the steric effect entirely inhibits the formation of the supramolecular associates - a phenomenon commonly observed and thoroughly studied in aliphatic systems. In fact, XRD investigations have shown no clear pre-peak feature in the low scattering vector region of diffractograms for PhBs, suggesting their local structure to be disordered like in ordinary liquids. On the other hand, in ABs there was a strong pre-peak in the diffraction patterns, indicating the formation of the H-bonded associates and medium-range order. Such a picture of the nanoscale organization through H-bonding in both groups of alcohols could be misleading as FTIR and dielectric data showed that the phenyl moiety has only a very small impact on the strength of H-bonds and the association process. Importantly, it was found that Kirkwood factors are much higher than the unity for both ABs and PhBs and not so much different from each other. This finding, together with the data analysis according to the Jadżyn and Świergiel approach [39], clearly indicated that associates with rather the chain-like organization of H-bonds are formed in the studied systems, irrespective of the presence of phenyl moiety.

Our studies also revealed that the location of the hydroxyl unit (either it is attached to the primary and secondary carbon) has a more prominent effect on the H-bonding pattern than the steric hindrance posed by the aromatic group. We found the series of systematic deviations between primary and secondary alcohols, which includes much higher glass transition temperature, Kirkwood factor, activation enthalpy of the dissociation process, as well as smaller H-bond strength and more homogeneity of the H-bonded network in the latter materials with respect to the former ones. It signifies a direct correlation between the self-assembly ability of the butanol isomers and their molecular geometry (the hydroxyl group's location within the carbon skeleton), which highly influences the aggregation of these systems. Thus, a combination of outcomes from all experimental techniques allowed us to understand better the relationships between the structural static and dynamic properties of the studied alcohols.

CRediT authorship contribution statement

B. Hachuła: Writing - original draft, Formal analysis, Methodology, Conceptualization. **J. Grelska:** Investigation. **N. Soszka:** Investigation, Formal analysis. **K. Jurkiewicz:** Writing - original draft, Investigation, Formal analysis, Visualization. **A. Nowok:** Investigation. **A.Z. Szeremeta:** Investigation. **S. Pawlus:** Investigation, Funding acquisition. **M. Paluch:** Supervision. **K. Kaminski:** Methodology, Supervision.

Declaration of Competing Interest

The authors declare that they have no known competing financial interests or personal relationships that could have appeared to influence the work reported in this paper.

Acknowledgment

B.H, J.G, K.J., K.K., and S.P. are thankful for the Polish National Science Centre's financial support within the OPUS project (Dec. no UMO-2019/35/B/ST3/02670). K.J. is grateful for the financial support from the Foundation for Polish Science within the START program.

Appendix A. Supplementary material

Supplementary data to this article can be found online at https://doi.org/10.1016/j.molliq.2021.117098.

References

[1] R. Böhmer, C. Gainaru, R. Richert, Structure and dynamics of monohydroxy alcohols-Milestones towards their microscopic understanding, 100 years after Debye, Phys. Rep. 545 (2014) 125–195, https://doi.org/10.1016/j.physrep.2014.07.005.
[2] N.Y. Tan, R. Li, P. Bräuer, C. D'Agostino, L.F. Gladden, J.A. Zeitler, Probing hydrogen-bonding in binary liquid mixtures with terahertz time-domain spectroscopy: A comparison of debye and absorption analysis, Phys. Chem. Chem. Phys. 17 (8) (2015) 5999–6008, https://doi.org/10.1039/C4CP04477K.
[3] T. Kulschewski, J. Pleiss, Binding of Solvent Molecules to a Protein Surface in Binary Mixtures Follows a Competitive Langmuir Model, Langmuir 32 (35) (2016) 8960–8968, https://doi.org/10.1021/acs.langmuir.6b0254610.1021/acs.langmuir.6b02546.s001.
[4] R. Ghosh, S. Roy, B. Bagchi, Solvent sensitivity of protein unfolding: Dynamical study of chicken villin headpiece subdomain in water-ethanol binary mixture, J. Phys. Chem. B. 117 (49) (2013) 15625–15638, https://doi.org/10.1021/jp406255z.
[5] M. Vraneš, N. Cvjetićanin, S. Papović, B. Šarac, I. Prislan, P. Megušar, S. Gadžurić, M. Bešter-Rogač, Electrical, electrochemical and thermal properties of the ionic liquid + lactone binary mixtures as the potential electrolytes for lithium-ion batteries, J. Mol. Liq. 243 (2017) 52–60, https://doi.org/10.1016/j.molliq.2017.07.129.
[6] P. Marín, S. Ordóñez, F.V. Díez, Combustion of toluene-hexane binary mixtures in a reverse flow catalytic reactor, Chem. Eng. Sci. 63 (20) (2008) 5003–5009, https://doi.org/10.1016/j.ces.2008.03.001.
[7] T.S. Kang, K. Ishiba, M.-A. Morikawa, N. Kimizuka, Self-assembly of azobenzene bilayer membranes in binary ionic liquid-water nanostructured media, Langmuir 30 (9) (2014) 2376–2384, https://doi.org/10.1021/la405010f.
[8] T. Nakashima, N. Kimizuka, Kimizuka, Vesicles in salt: Formation of bilayer membranes from dialkyldimethylammonium bromides in ether-containing ionic liquids, Chem. Lett. 31 (10) (2002) 1018–1019, https://doi.org/10.1246/cl.2002.1018.
[9] K.M. Murdoch, T.D. Ferris, J.C. Wright, T.C. Farrar, Infrared spectroscopy of ethanol clusters in ethanol-hexane binary solutions, J. Chem. Phys. 116 (13) (2002) 5717–5724, https://doi.org/10.1063/1.1458931.
[10] S. Stehle, A.S. Braeuer, Hydrogen Bond Networks in Binary Mixtures of Water and Organic Solvents, J. Phys. Chem. B. 123 (2019) 4425–4433, https://doi.org/10.1021/acs.jpcb.9b02829.
[11] A. Wakisaka, T. Ohki, Phase separation of water-alcohol binary mixtures induced by the microheterogeneity, Faraday Discuss. 129 (2005) 231–245, https://doi.org/10.1039/b405391e.
[12] P. Tomza, W. Wrzeszcz, S. Mazurek, R. Szostak, M.A. Czarnecki, Microheterogeneity in binary mixtures of water with CH3OH and CD3OH: ATR-IR spectroscopic, chemometric and DFT studies, Spectrochim. Acta - Part A Mol. Biomol. Spectrosc. 197 (2018) 88–94, https://doi.org/10.1016/j.saa.2018.01.068.
[13] S. Lotze, C.C.M. Groot, C. Vennehaug, H.J. Bakker, Femtosecond mid-infrared study of the dynamics of water molecules in water-acetone and water-dimethyl sulfoxide mixtures, J. Phys. Chem. B. 119 (16) (2015) 5228–5239, https://doi.org/10.1021/jp512703w.
[14] M. Raveendra, M. Chandrasekhar, K. Chandrasekhar Reddy, A. Venkatesulu, K. Sivakumar, K. Dayananda Reddy, Study on thermo physical properties of binary mixture containing aromatic alcohol with aromatic, substituted aromatic amines at different temperatures interms of FT-IR, 1H NMR spectroscopic and DFT method, Fluid Phase Equilib. 462 (2018) 85–99, https://doi.org/10.1016/j.fluid.2018.01.025.
[15] F. Pabst, J. Gabriel, T. Blochowicz, Mesoscale Aggregates and Dynamic Asymmetry in Ionic Liquids: Evidence from Depolarized Dynamic Light Scattering, J. Phys. Chem. Lett. 10 (9) (2019) 2130–2134, https://doi.org/10.1021/acs.jpclett.9b00686.
[16] R. Häkkinen, O. Alshammari, V. Timmermann, C. D'Agostino, A. Abbott, Nanoscale Clustering of Alcoholic Solutes in Deep Eutectic Solvents Studied by Nuclear Magnetic Resonance and Dynamic Light Scattering, ACS Sustain. Chem. Eng. 7 (2019) 15086–15092. Doi: 10.1021/acssuschemeng.9b03771.
[17] J. Troncoso, K. Zemánková, A. Jover, Dynamic light scattering study of aggregation in aqueous solutions of five amphiphiles, J. Mol. Liq. 241 (2017) 525–529, https://doi.org/10.1016/j.molliq.2017.06.022.
[18] A. Ghoufi, Molecular origin of the prepeak in the structure factor of alcohols, J. Phys. Chem. B. 124 (50) (2020) 11501–11509, https://doi.org/10.1021/acs.jpcb.0c09302.
[19] J.L. MacCallum, D.P. Tieleman, Structures of neat and hydrated 1-octanol from computer simulations, J. Am. Chem. Soc. 124 (50) (2002) 15085–15093, https://doi.org/10.1021/ja027422o.
[20] A. Mariani, P. Ballirano, F. Angiolari, R. Caminiti, L. Gontrani, Does High Pressure Induce Structural Reorganization in Linear Alcohols? A Computational Answer, ChemPhysChem 17 (19) (2016) 3023–3029, https://doi.org/10.1002/cphc.201600268.
[21] W. Dannhauser, Dielectric study of intermolecular association in isomeric octyl alcohols, J. Chem. Phys. 48 (5) (1968) 1911–1917, https://doi.org/10.1063/1.1668989.
[22] K. Jurkiewicz, B. Hachuła, E. Kamińska, K. Grzybowska, S. Pawlus, R. Wrzalik, K. Kamiński, M. Paluch, Relationship between Nanoscale Supramolecular Structure, Effectiveness of Hydrogen Bonds, and Appearance of Debye Process, J. Phys. Chem. C. 124 (4) (2020) 2672–2679, https://doi.org/10.1021/acs.jpcc.9b0980310.1021/acs.jpcc.9b09803.s001.
[23] M. Požar, A. Perera, On the existence of a scattering pre-peak in the mono-ols and diols, Chem. Phys. Lett. 671 (2017) 37–43, https://doi.org/10.1016/j.cplett.2017.01.014.
[24] T. Büning, J. Lueg, J. Bolle, C. Sternemann, C. Gainaru, M. Tolan, R. Böhmer, Connecting structurally and dynamically detected signatures of supramolecular Debye liquids, J. Chem. Phys. 147 (23) (2017) 234501, https://doi.org/10.1063/1.4986866.
[25] M. Tomšič, J. Cerar, A. Jamnik, Supramolecular structure vs. rheological properties: 1,4–Butanediol at room and elevated temperatures, J. Colloid Interface Sci. 557 (2019) 328–335, https://doi.org/10.1016/j.jcis.2019.09.020.
[26] M. Požar, J. Bolle, C. Sternemann, A. Perera, On the X-ray Scattering Pre-peak of Linear Mono-ols and the Related Microstructure from Computer Simulations, J. Phys. Chem. B. 124 (38) (2020) 8358–8371, https://doi.org/10.1021/acs.jpcb.0c05932.
[27] L. Almásy, A.I. Kuklin, M. Požar, A. Baptista, A. Perera, Microscopic origin of the scattering pre-peak in aqueous propylamine mixtures: X-ray and neutron experiments: Versus simulations, Phys. Chem. Chem. Phys. 21 (18) (2019) 9317–9325, https://doi.org/10.1039/C9CP01137D.
[28] A. Hédoux, Y. Guinet, L. Paccou, P. Derollez, F. Danède, Vibrational and structural properties of amorphous n-butanol: A complementary Raman spectroscopy and X-ray diffraction study, J. Chem. Phys. 138 (21) (2013) 214506, https://doi.org/10.1063/1.4808159.
[29] V.A. Durov, I.Y. Shilov, O.G. Tereshin, Modeling of supramolecular structure and dielectric properties of butanols from melting point to supercritical state, J. Phys. Chem. B. 112 (27) (2008) 8076–8083, https://doi.org/10.1021/jp710428n.
[30] S. Choi, S. Parameswaran, J.-H. Choi, Effects of molecular shape on alcohol aggregation and water hydrogen bond network behavior in butanol isomer solutions, Phys. Chem. Chem. Phys. 23 (23) (2021) 12976–12987, https://doi.org/10.1039/D1CP00634G.
[31] K.S. Vahvaselkä, R. Serimaa, M. Torkkeli, Determination of Liquid Structures of the Primary Alcohols Methanol, Ethanol, 1-Propanol, 1-Butanol and 1-Octanol by X-ray Scattering, J. Appl. Crystallogr. 28 (2) (1995) 189–195, https://doi.org/10.1107/S0021889894010149.
[32] T. Böhmer, J.P. Gabriel, T. Richter, F. Pabst, T. Blochowicz, Influence of Molecular Architecture on the Dynamics of H-Bonded Supramolecular Structures in Phenyl-Propanols, J. Phys. Chem. B. 123 (51) (2019) 10959–10966, https://doi.org/10.1021/acs.jpcb.9b07768.
[33] K. Jurkiewicz, S. Kołodziej, B. Hachuła, K. Grzybowska, M. Musiał, J. Grelska, R. Bielas, A. Talik, S. Pawlus, K. Kamiński, M. Paluch, Interplay between structural static and dynamical parameters as a key factor to understand peculiar behaviour of associated liquids, J. Mol. Liq. 319 (2020) 114084, https://doi.org/10.1016/j.molliq.2020.114084.
[34] M. Mons, E.G. Robertson, J.P. Simons, Intra- and Intermolecular π-Type Hydrogen Bonding in Aryl Alcohols: UV and IR-UV Ion Dip Spectroscopy, J. Phys. Chem. A. 104 (2000) 1430–1437, https://doi.org/10.1021/jp993178k.

[35] O. Takahashi, K.o. Saito, Y. Kohno, H. Suezawa, S. Ishihara, M. Nishio, The conformation of alkyl benzyl alcohols studied by ab initio MO calculations - A comparison with IR and NMR spectroscopic data, European J. Org. Chem. 2004 (11) (2004) 2398–2403, https://doi.org/10.1002/ejoc.200300801.
[36] M. Hassaine, PhD thesis, Calorimetric and thermodynamic study of molecular glasses and crystals of butanol, Universidad Autónoma de Madrid, Department of Condensed Matter Physics, 2013.
[37] F. Kremer, A. Schönhals, Broadband dielectric spectroscopy, first ed., Springer Science & Business Media, New York, 2002.
[38] H. Fröhlich, Theory of Dielectrics, 2nd ed., Clarendon Press, Oxford, 1958.
[39] J. Jadżyn, J. Świergiel, Mesoscopic clustering in butanol isomers, J. Mol. Liq. 314 (2020) 113652, https://doi.org/10.1016/j.molliq.2020.113652.
[40] W. Dannhauser, R.H. Cole, Dielectric properties of liquid butyl alcohols, J. Chem. Phys. 23 (10) (1955) 1762–1766, https://doi.org/10.1063/1.1740576.
[41] S. Bauer, H. Wittkamp, S. Schildmann, M. Frey, W. Hiller, T. Hecksher, N.B. Olsen, C. Gainaru, R. Böhmer, Broadband dynamics in neat 4-methyl-3-heptanol and in mixtures with 2-ethyl-1-hexanol, J. Chem. Phys. 139 (13) (2013) 134503, https://doi.org/10.1063/1.4821229.
[42] S. Pawlus, M. Wikarek, C. Gainaru, M. Paluch, R. Böhmer, How do high pressures change the Debye process of 4-methyl-3-heptanol?, J Chem. Phys. 139 (6) (2013) 064501, https://doi.org/10.1063/1.4816364.
[43] R. Hayes, G.G. Warr, R. Atkin, Structure and Nanostructure in Ionic Liquids, Chem. Rev. 115 (13) (2015) 6357–6426, https://doi.org/10.1021/cr500411q.
[44] T. Cosby, Z. Vicars, Y. Wang, J. Sangoro, Dynamic-Mechanical and Dielectric Evidence of Long-Lived Mesoscale Organization in Ionic Liquids, J. Phys. Chem. Lett. 8 (15) (2017) 3544–3548, https://doi.org/10.1021/acs.jpclett.7b0151610.1021/acs.jpclett.7b01516.s001.
[45] T. Sonnleitner, D.A. Turton, S. Waselikowski, J. Hunger, A. Stoppa, M. Walther, K. Wynne, R. Buchner, Dynamics of RTILs: A comparative dielectric and OKE study, J. Mol. Liq. 192 (2014) 19–25, https://doi.org/10.1016/j.molliq.2013.09.019.
[46] O. Russina, A. Triolo, L. Gontrani, R. Caminiti, Mesoscopic Structural Heterogeneities in Room-Temperature Ionic Liquids, J. Phys. Chem. Lett. 3 (1) (2012) 27–33, https://doi.org/10.1021/jz201349z.
[47] D.A. Turton, J. Hunger, A. Stoppa, G. Hefter, A. Thoman, M. Walther, R. Buchner, K. Wynne, Dynamics of Imidazolium Ionic Liquids from a Combined Dielectric Relaxation and Optical Kerr Effect Study: Evidence for Mesoscopic Aggregation, J. Am. Chem. Soc. 131 (31) (2009) 11140–11146, https://doi.org/10.1021/ja903315v.